Stony Brook University

Regulation of Interferon Stimulated Gene 54-mediated Apoptosis by Antioxidants PRDX5 and SOD2

A Thesis Presented

by

Mel Pilar Espaillat

to

The Graduate School

in Partial Fulfillment of the

Requirements

for the Degree of

Master of Science

in

Biochemistry and Cell Biology

Stony Brook University

August 2012

Stony Brook University

The Graduate School

Mel Pilar Espaillat

We, the thesis committee for the above candidate for the

Master of Science degree, hereby recommend

acceptance of this thesis.

Nancy C. Reich Marshall, Ph.D.
Professor, Molecular Genetics and Microbiology

Laurie Krug, Ph.D.
Assistant Professor, Molecular Genetics and Microbiology

This thesis is accepted by the Graduate School

Charles Taber
Interim Dean of the Graduate School

Abstract of the Thesis

Regulation of Interferon Stimulated Gene 54-mediated Apoptosis by Antioxidants PRDX5 and SOD2

by

Mel Pilar Espaillat

Master of Science

in

Biochemistry and Cell Biology

Stony Brook University

2012

Interferons (IFNs) are the most potent mediators of antiviral activities in the immune system. Viral molecular patterns are detected by receptors of the innate immune system, resulting in IFN production and subsequent IFN-stimulated gene (ISG) expression. The production of IFN serves as a danger signal that triggers a cascade of molecular events in the cell for the induction of antiviral mechanisms. The ISG products protect cells against viral replication, induce anti-proliferative mechanisms, and modulate the development of innate and adaptive immunity. The expression of ISG54 is mediated by type I IFN signaling and results in induction of apoptosis via a mitochondrial pathway. To understand the molecular mechanism underlying this activity, we aimed to identify molecular partners of the gene product, p54. Two antioxidant enzymes were identified from a yeast two-hybrid assay, peroxiredoxin 5 (PRDX5) and superoxide dismutase 2 (SOD2). To confirm the interaction between these proteins and p54, we cloned the cDNA of both genes and confirmed their interaction with p54 by co-immunoprecipitation and Western

blot. In addition, we tested if these antioxidants could regulate ISG54-mediated apoptosis. Apoptosis was assessed using flow cytometric analysis of cells co-transfected with ISG54 with or without PRDX5 and SOD2 and co-stained with Annexin-V and propodium iodide (PI). In this report we show that both enzymes can transiently inhibit ISG54-mediated apoptosis. The results describe novel findings in the molecular mechanism of ISG54 cellular activity.

Dedication Page

I dedicate this thesis to one who has decided to walk this road by my side

JL

Table of Contents

List of Figures

List of Abbreviations

2-5’ OAS	2-5’ oligoadenylate synthetase
AP-1	activator protein 1
CARD	caspase recruitment domain
CDK	cyclin dependent kinase
CKI	CDK inhibitors
CpG	cytosine-phosphate-guanosine
DC	dendritic cells
dsRNA	double stranded RNA
GAF	γ activating factor
GEF	guanine nucleotide exchange factors
HSP	heat shock protein
IFIT	type I IFN-induced protein with tetratricopeptide repeats
IFN	interferon
IKK	IκB kinase
IPS-1	interferon β promoter stimulator-1
IRAK	interleukin-1 receptor associated kinase
IRF	interferon regulatory factors
ISG	interferon stimulated genes
ISGF3	interferon stimulated gene factor 3
ISRE	interferon stimulated response element
IκB	inhibitor or NFκB
JAK	Janus activated kinase
LPG2	laboratory of genetics and physiology 2
MAPK	mitogen-activated protein kinase
Mda5	melanoma differentiation-associated factor 5
MHC	major histocompatibility complex
MTS	mitochondria targeting sequence
NFκB	nuclear factor kappa-light-chain-enhancer of activated B cells
NOD2	nucleotide-binding oligomerization domain 2
PAMP	pathogen-associated molecular patterns
PCR	polymerase chain reaction
PI	propidium Iodide
PKR	protein kinase RNA-activated
PRD	positive regulatory domain
PRDX	peroxiredoxin
PRR	pattern recognition receptors
RIG-I	retinoic acid-inducible gene I

RLR	RIG-I-like receptor
RNase	ribonuclease
SH2	Src homology 2 domain
SOD	superoxide dismutase
ssRNA	single stranded RNA
STAT	signal transducer and activator of transcription
STING	stimulator of interferon genes
TAB1	TAK1 binding protein 1
TAK1	TGF-β activated kinase 1
TANK	TRAF family member-associated NFκB activator
TBK1	TANK-binding kinase 1
TCR	T cell receptor
TGF-β	tumor growth factor β
TIR	Toll/IL-1 receptor
TPR	tetratricopeptide repeat
TRAF3	tumor necrosis factor receptor associated factor 3
TRIF	TIR domain-containing adaptor protein inducing IFN-β
TRIM25	tripartite motif 25
VSIG	virus stress-inducible genes

Acknowledgments

This work would have not been possible without the training and assistance of Dr. Marcin Stawowczyk, Ha-Youn Shin, Dr. Velasco Cimica, Dr. Jane Foreman, and Tiffany Lay.

INTRODUCTION

The immune system has devised an array of strategies to guard and protect against pathogenic intruders. In the context of viruses, interferons (IFNs) are the signaling molecules at the vanguard of infection. These cytokines play a key role in innate immunity by promoting a rapid response to inhibit viral replication, as well as regulating the transition to adaptive immunity for complete clearance and long term protection. The antiviral mechanisms of IFNs are mediated by the expression of genes and regulation of immune activities to confer protection against these pathogens. The hundreds of genes activated by these cytokines influence a diverse number of biological functions and target multiple aspects of viral infection, such as penetration, viral genome replication, and synthesis of viral progeny (*1*).

IFNs are a big family of cytokines classified as type I, II and III based on sequence homology, receptor specificity and function. Type I IFN is the first class expressed during a viral infection and includes the most members: 14-20 subtypes of IFN-α (varying among species), one type of IFN-β (*2*), IFN-ω, IFN-κ, IFN-ε, IFN-δ, and IFN-τ (*3*); type II includes a single member, IFN-γ, and the last class is type III, consisting of IFN-λ1, IFN-λ2, IFN-λ3 (*4*) (*5*).

TYPE I IFN

Each subtype of type I IFN is encoded by its own gene, with all intron-less genes located in human chromosome number 9 (*3*). The expression of different subtypes is differentially regulated by individual promoters and distal regulatory regions. Type I IFNs are part of the first wave of cytokines rapidly produced during viral infection. Viral pathogen-associated molecular patterns (PAMPs), such as double stranded RNA (dsRNA) and viral proteins, serve as molecular signatures of viruses and are recognized by particular pattern recognition receptors (PRR) of the

innate immune system. Upon detection and binding of a viral PAMP, these sensors trigger the activation of transcription factors to induce production of type I IFN. Transcription of type I IFN is activated by various transcription factors: interferon regulatory factors (IRFs), nuclear factor kappa-light-chain-enhancer of activated B cells (NFκB), and activator protein 1 (AP-1) (Fig 1) (*6*). The transcription factors bind positive regulatory domains (PRD) located on the promoter of IFN-β gene, while the promoters of IFN-α genes only bind IRFs (*1*).

TRANSCRIPTION FACTORS INVOLVED IN TYPE I IFN PRODUCTION

Two members of the IRF family, IRF3 and IRF7, are indispensable in promoting the antiviral response of IFN signaling. IRF3 is constitutively expressed by all cells and translocates in and out of the nucleus. Unphosphorylated IRF3 resides primarily in the cytoplasm due to an increased rate of nuclear export versus import. The transcription factor becomes activated in the cytoplasm by serine phosphorylation, allowing it to bind nuclear acetyltransferases CREB binding protein (CBP) and p300, forming the complex dsRNA-activated factor 1 (DRAF1) to induce transcription (*7*). Activation of IRF3 occurs early in the IFN pathway to induce expression of type I IFN-α4 and IFN-β. Signaling of early type I IFN induces the formation of interferon stimulated gene factor 3 (ISGF3) complex. Consequently, ISGF3 promotes the expression of IRF7, which in turn activates the transcription of additional genes (*8*).

NFκB family is composed of five members: RelA, RelB, c-Rel, NFκB1 and NFκB2. NFκB1 and NFκB2 are synthesized as precursors p105 and p100, respectively. The precursor proteins undergo proteolytic processing to generate the respective mature protein subunits p50 and p52 (*9*). The transcription factors homo- or heterodimerize to form the mature transcription factor. P50 and RelA dimer is most frequently involved in the production of type I IFN by PRR signaling. The transcription factor is kept inactive in the cytoplasm by interaction with a member

of the inhibitor or NFκB (IκB) family (*2*). IκB members can restrict NFκB in the cytoplasm by blocking its nuclear localization signal. The inhibition can be reversed by phosphorylation of the inhibitor complex performed by IκB kinase (IKK). The IKK complex is composed of subunits IKKα, IKKβ and IKKγ (also known as NEMO). Phosphorylated IκB gets polyubiquitinated and degraded by the proteasome (*10*).

The transcription factor AP-1 is a heterodimer composed of c-Jun and activated transcription factor-2 (ATF-2). The components of AP-1 are activated by the mitogen-activated protein kinase (MAPK) p38 and c-Jun NH2-terminal kinase (JNK). AP-1 can bind promoters of target genes prior to its phosphorylation, and become trans-activated once bound. AP-1 activates expression of IFN-β by binding to the positive regulatory domain IV (PRDIV) site-also known as c-AMP responsive element (CRE)-located in the IFN-β enhancer (*2*).

PRR SIGNALING

Out of the numerous PRR patrolling for microorganism, two categories play a crucial role in the production of type I IFN: Toll-like receptors (TLRs) and the cytoplasmic retinoic acid-inducible gene I (RIG-I)-like receptor (RLR) family (Fig 1) (*11*) (*12*). In addition to implementing a rapid danger alarm, PRR ligation induces the secretion of pro-inflammatory cytokines that lead to the activation of antigen-presenting cells, such as dendritic cells (DC), and subsequent transition to adaptive immunity (*12*). The manifold distribution of PRR employed to survey pathogens induce signaling transduction pathways that can have redundant or synergistic functions to assure rapid and strategic execution of antiviral responses.

TLR SIGNALING

The TLR family is composed of transmembrane glycoprotein receptors, with 10 different members identified in humans and 12 members in mice. TLRs are characterized by an N-terminal PAMP binding region containing leucine-rich repeats that face the extracellular environment when localized in the plasma membrane or the lumen of intracellular compartments, such as, the endoplasmic reticulum (ER) and endosomes (*13*). The C-terminal region of TLRs has a Toll/IL-1 receptor (TIR) domain that mediates intracellular signaling. Out of several TLRs involved in virus recognition and type I IFN production, 4 types (TLR3, TLR7, TLR8, and TLR9) are known to recognize viral nucleic acid delivered to endosome vesicles (*14*). TLRs can also reside on the plasma membrane where they detect viral envelope glycoproteins and other PAMPS (*6*). PAMPS can be delivered to endosomes by endocytosis of extracellular viral particles or by autophagy. Autophagy is a mechanism by which cells can autodigest organelles and cytosolic molecules to maintain cellular homeostasis (*13*).

Production of type I IFN induced by TLR3 signaling is activated by dsRNA. The antiviral properties of TLR3 have been attributed to particular cells, notably phagocytic CD8α+ CD4- dendritic cells (DCs). TLR3 activation induces the expression of IFN-β and certain subtypes of IFN-α (*2*). The signaling is dependent on the recruitment of TIR domain-containing adaptor protein inducing IFN-β (TRIF) for downstream activation of IRF3. TRIF interacts with tumor necrosis factor receptor associated factor 3 (TRAF3) that scaffolds TRIF with the kinase TRAF family member-associated NFκB activator (TANK)-binding kinase 1 (TBK1). TBK1 associates with IKKε for phosphorylation of IRF3 (*13*). IRF3 cooperates with NFκB and AP-1 to form the enhanceosome to induce gene expression of IFN-β. In experiments using the viral dsRNA analogue, polyIC, TRAF3-knockout mice fail to induce IFN-β production (*15*). In addition to the

dependence of the adaptor TRIF, the downstream effectors, TRAF3 and TBK1, play essential roles in this pathway. Overexpression of a TBK1 mutant that is deficient of its kinase activity inhibited TRIF-dependent activation of IFN-β promoter (*10*). By a positive feedback loop mechanism, production of this first wave of type I IFN induces the expression of IRF7. IRF7 gets activated by the TBK1/IKKε complex to amplify the expression of other type I IFNs.

TLR7 and TLR8 are phylogenetically and functionally similar, but their anti-viral specificity differs between species. Human TLR8, but not the orthologue in mice, recognizes human immunodeficiency virus (HIV). TLR8 is expressed mainly in myeloid DC and monocytes while TLR7 is expressed in plasmacytoid dendritic cells (pDC), and B cells (*6*). TLR7, TLR8 and TLR9 induce the expression of type I IFN and inflammatory cytokines using the essential adaptor protein myeloid differentiation primary response gene 88 (Myd88). TLR7/TLR8 recognize single stranded RNA (ssRNA), whereas TLR9 binds to viral DNA with unmethylated 2'deoxyribo cytosine-phosphate-guanosine (CpG)-containing DNA motifs (*13*). Plasmacytoid dendritic cells (pDC), also known as IFN-producing DCs, produce large amounts of type I IFN via TLR7-mediated IRF7 activation. The ability of TLR7 to induce great amounts of type I IFN is due to the constitutive expression of TLR7 in pDC and its localization in the endosome. In unstimulated cells, TLR7 is localized to the ER. Upon its activation, TLR7 is delivered to the endosome and it is retained for extended periods before its degradation (*6*).

TLR7, TLR8 and TLR9 induce the activation of transcription factors NFκB and AP-1 for expression of type I IFN. The adaptor protein for TLR7-TLR9, Myd88, has two domains. Myd88 homotypic interaction with TLR7-TLR9 is mediated via the C-terminal TIR domain. Through the N-terminal death domain, Myd88 interacts with kinases belonging to the interleukin-1 receptor associated kinases (IRAK), IRAK1 and IRAK4. IRAK4 phosphorylates IRAK1,

allowing it to dissociate from Myd88 and interact with TRAF6, a RING-domain E3 ubiquitin ligase. TRAF6 signals downstream to activate the IKKα complex, which in turn phosphorylates IRFs that induce expression of IFN-α. TRAF6 can also ubiquitinate the MAP3 kinase member tumor growth factor β (TGF-beta) activated kinase 1 (TAK1) and NEMO. This results in the activation of the two additional transcription factors implicated in type I IFN expression: NFκB and AP-1. TAK1 associates with its binding proteins, TAK1 binding protein 1 (TAB1), TAB2, and TAB3. The TAK1/TABs complex phosphorylates one of the components of the IKK complex, IKKβ, to activate it and induce degradation of IκB and subsequent activation NFκB expression. Lastly, the activation of the MAPK cascade pathway by the TAK1/TABs complex can also activate the transcription factor AP-1(*10*).

Other IRFs in addition to IRF3 and IRF7 are involved in the production of type I IFN. IRF8 abrogates production of type I IFN via TLR9 pathway (*10*). IRF8 is involved in NFκB signaling via TLR9 (*16*) mediating IFN-α secretion in pDC (*17*). In addition, IRF8 plays an important role in the second wave of type I IFN production (*10*). The role of IRFs in the production of IFN can be particular to specific cell types, such as in the case of IRF1 and IRF5, which bind to Myd88 to regulate IFN-β production in conventional DC (cDC) but not in pDC (*10*).

RLR SIGNALING

RLR are RNA helicases that play an important role in the recognition of cytoplasmic viral RNA to signal type I IFN production. There are three types of RLR involved in IFN signaling: retinoic acid inducible gene 1 (RIG-1), melanoma differentiation-associated factor 5 (Mda5) and laboratory of genetics and physiology 2 (LPG2) (*6*). RIG-I and Mda5 have different specificity for RNA virus recognition. RIG-1 can differentiate viral from host RNA due to 5’ end modification. Unlike host RNA which contains a 5’ cap, viral RNA is usually uncapped and

displays a 5’ end triphosphate that serves as a PAMP for RLR recognition (*14*). Mda5 recognizes dsRNA and unwinds the structure via its helicase activity (*10*). LPG2 serves as a regulator of the antiviral activities of RIG-1 and Mda5 (*10*).

RLR signaling is mediated via adaptor protein interferon β promoter stimulator-1 (IPS-1). The adaptor IPS-1 contains a caspase recruitment domain (CARD)-like region that mediates the homotypic interaction with RIG-I and Mda5. The signaling pathway of RIG-1 and Mda5 mediated by IPS-1 ultimately activates IRF3 for type I IFN production. Ligation of RIG-1 causes a conformational change allowing the CARD domain to be exposed and polyubiquitinated by the E3 ubiquitin ligase tripartite motif 25 (TRIM25). The polyubiquitination of RIG-I allows IPS-1 to bind and the complex formed interacts with TRAF3 (*6*). TRAF3 subsequently activates TBK-1/IKKi and the IKK complex for induction of IFN-β via IRF3 activation and NFκB nuclear localization, respectively (*11*) (*10*).

Nucleotide-binding oligomerization domain 2 (NOD2) is a PRR that primarily recognizes bacterial peptidoglycan. NOD2 has also been identified as a sensor of ssRNA and inducer of type I IFN by signaling via the RIG-1 pathway (*6*). Additionally, the adaptor protein stimulator of interferon genes (STING) that localizes in the ER and the mitochondria, binds RIG-1 and IPS-1 and has been shown to induce IFN-β production triggered by viral DNA (*6*) (*12*).

TYPE II IFN

Type II IFN (IFN-γ) is not induced immediately following viral antigen recognition, but as a part of a second wave of cytokines. Unlike type I IFN-that is produced by almost every nucleated cell- type II IFN is mainly produced by immune cells and it plays an important role in the development of an adaptive response (*14*). NK cells, T cells, DCs, and macrophages are the main

producers of this cytokine. In T cells, activation of the T cell receptor (TCR) by antigen presenting cells (APC) or by cytokine stimulation induces the expression of type II IFN.

The transcription factors involved in type II IFN expression include NFκB, AP-1, and members of the STAT family. Many cytokines work synergistically to induce the expression of type II IFN, important ones are type I IFN, IL-12 and IL-18. The combination of transcription factors necessary to induce IFN-γ expression depends on the cell type and stimulant (*2*).

TYPE I IFN SIGNALING

The expression of type I IFN initiates an alarm to communicate to other innate immune cells of the presence of danger. Upon their production, type I IFNs are secreted and can signal in a paracrine or autocrine fashion by signaling through specific receptors. Receptor ligation initiates a signal transduction that culminates in the transcription of interferon stimulated genes (ISG) (*1*).

All type I IFNs bind a common receptor composed of two subunits: IFNAR1 and IFNAR2. The multi-chain receptor lacks intrinsic kinase activity and associates with two members of the family of Janus activated kinases (JAK), TYK2 and JAK1 (Fig 2). The JAKs are tyrosine kinases that become activated upon receptor ligation. As a result of IFN binding, the receptor rearranges causing the JAKs to position in an optimal conformation allowing a cross-phosphorylation of tyrosine residues in the activation loop of JAKs. The transcription factors signal transducer and activator of transcription (STAT) are the next elements involved in the signal relay. Two members, STAT1 and STAT2, are recruited by their Src homology 2 domain (SH2) to the phosphotyrosine residues (*18*). The STATs are subsequently phosphorylated by JAKs triggering their activation and dimerization. Activated STATs associate with IRF-9, forming ISGF3 (Fig 2). The transcription factor complex binds interferon stimulated response element (ISRE) (*8*), an

enhancer element in the promoter of all type I IFN genes, and binding of ISGF3 initiates transcription of ISG (*19*).

Of the different MAPK pathways, the p38 cascade plays the most significant role in IFN induced activities. Inhibition of this pathway can abrogate IFN-α-mediated gene transcription. The activation of the MAPK pathway occurs independently of STAT activation. Activated JAKs can alternatively phosphorylate guanine nucleotide exchange factors (GEFs) that activate small GTPases, such as RAC1 that can activate p38. P-38 dependent signaling pathway has been shown to be crucial for the anti-proliferative properties of type I IFN signaling and anti-viral actions by IFN-α in certain viruses such as hepatitis C and vesicular stomatitis virus (*3*).

TYPE II IFN SIGNALING

Type II IFN signaling can be activated through the classical JAK-STAT pathway by binding receptors IFNGR1 and IFNGR2. The type II IFN receptors associate with JAK1 and JAK2, that regulate by phosphorylation the activation and formation of the STAT1 homodimer (Fig 2), originally called γ activating factor (GAF). The STAT1 homodimer binds IFN-γ activated sites (*20*) located in the promoter of IFN-γ responsive ISGs. The signaling pathways of both type I and type II IFN can overlap adding to the complexity of IFN signaling. For example, type I IFN can also induce the formation of the STAT1 homodimer to signal by binding to GAS elements (*3*), while type II IFN can also promote production of type I IFN by activating ISGF3 (*21*).

TYPE III IFN SIGNALING

There are three different subclasses of type III IFN (IFN-λ) in humans, IFN-λ1-3. Type III IFNSs signals through a dimeric receptor composed of IFN-λR1 chain (also known as IL-28AR) and the IL-10R2 chain. “Both type I and type III IFNs stimulate common signaling pathways, consisting

of the activation of Jak1 and Tyk2 kinases (Fig 2) and leading to the activation of ISGF3 transcription complex" (*4*).

CELLULAR FUNCTIONS REGULATED BY IFN

Activation of innate immunity serves as the initial danger alarm in the attempt to control infection until the artillery of adaptive immunity is implemented. Amongst their key role as antiviral mediators, IFNs regulate activities of innate and adaptive immune cells.

The antiviral effects are mediated directly by targeting different steps of the viral cycle: cell penetration, coat removal, transcription of nucleic acid, synthesis of proteins, and synthesis of progeny. Indirectly, IFN can mediate antiviral mechanisms by regulating different immune responses such as cell growth and development. By targeting different effectors and mechanism, the effect of IFN stimulation in cell is cumulative (*20*).

To successfully control the spread of viral infection, IFNs regulate the activation of adaptive immunity. The genes induced by IFN signaling alter the development and proliferative function of different cells to induce cell mediated immunity. This includes the maturation of antigen presenting cells by upregulating the expression of major histocompatibility complex (MHC) class I and class II molecules and the regulation of T cell activation (*8*). Antigen presentation to CD8 T cells via MHC class I activates cytotoxic T cell that can kill virus infected cells. In addition, IFN-γ regulates the proteasome machinery that processes antigen cleavage to increase peptide diversity for MHC loading (*21*). IFN-γ regulates the fate of leukocytes during viral infection by gearing CD4 T cells towards Th1 versus a Th2 direction. In addition, IFN-γ induces the expression of IL-12 by antigen presenting cells and upregulates expression of IL-12 receptor in CD4 T cells to promote the development of the Th1 response (*1*). Th1 cells are major

producers of IFN-γ, generating a positive feedback loop. Th1 response promotes the phagocytic activity of macrophages and the proliferation of cytotoxic T cells. IFN-γ also promotes B cell development and NK cell's cytotoxic activity. (*20*)

IFN regulates cell growth by targeting cellular factors that control the cell cycle. (*1*). IFN-γ can induce the expression of two cyclin dependent kinase (CDK) inhibitors (CKI) (p21 and p27) that arrest the cell cycle in the G1/S transition. Inhibition of the complex of cyclins and CDKs that regulate this checkpoint results in a downstream sequence of events where the tumor suppressor Rb is active. Rb inhibits the expression of oncogene c-Myc, a transcription factor that causes cell cycle progression. C-Myc can be alternatively regulated by targeting its co-activator Max; IFN-γ can increase the expression of Mad1, which can bind Max and sequester it from binding c-Myc (*21*).

INTERFERON STIMULATED GENES

IFNs regulate the expression of many genes to confer antiviral protection. Two enzymes play key roles in the antiviral mechanisms induced by IFN: protein kinase RNA-activated (PKR) and 2-5' oligoadenylate synthetase (2-5' OAS). The intermediate double stranded RNA (dsRNA) produced during viral nucleic acid replication functions as a co-factor for these enzymes (*1*).

PKR is a serine/threonine kinase induced by type I IFN; it becomes activated by autophosphorylation. Activated PKR phosphorylates the elongation factor eIF-2α, causing inhibition of viral protein synthesis (*14*). EIF-2α is a cofactor required for the recruitment of initiator methionine transfer RNA to the ribosome to form the translation pre-initiation complex. PKR is also involved in the regulation of various cellular activities, such as, apoptosis. PKR phosphorylates the protein kinase IKKβ that phosphorylates IκB, allowing NFκB to be activated

and bind target gene promoters to induce transcription. NFκB transcriptional regulation promotes the expression of pro-inflammatory cytokines TNF-α and IL-6. PKR induces apoptosis by regulating TNF-α splicing and via a Fas-dependent pathway (*1*).

One of the 2-5'OAS enzymes induced by type I IFN polymerizes ATP into 2-5' oligoadenylates that activate the ribonuclease (RNase) L. The ribonuclease can degrade viral mRNA, inhibiting the synthesis of viral proteins. RNase L can also induce apoptosis by binding and negatively regulating antiapoptotic proteins via a Bcl2-homology domain 3 (*1*).

The type I IFN-induced protein with tetratricopeptide repeats (IFIT) family consists of a group of virus stress-inducible genes (VSIGs). The members of this family are IFIT1 (ISG56), IFIT2 (ISG54), IFIT3 (ISG60), and IFIT4 (ISG58). All IFIT proteins are characterized by a tetratricopeptide repeat (TPR) motif formed by a degenerate 34 amino acid repeat sequence that only requires 8 to 9 residues to be conserved in key positions. The structural motif folds into two alpha antiparallel helices. The repeated motifs generate an amphiphatic right handed alpha bundle. The biochemical nature of the motif mediates protein-protein interaction and the formation of macromolecular complexes (*22*). The scaffolding property of the TPR motif has been studied in multiple cellular settings, such as, cell cycle regulation and protein transport (*23*). The TPR motif also regulates cellular activities as in the case of chaperone HSP (heat shock protein) 90 and HSP70, where the TPR motif of their adaptor proteins regulate their ATPase activity (*24*). One of the members, ISG56, is one of most induced genes in response to IFNs (*14*). This gene codes for the protein p56 which along with ISG54 product, p54, has been reported to interfere with translation of viral proteins by binding to components of the translation initiation factor eIF3 (*25*). In addition, ISG56 has been reported recently to mediate intrinsic immunity by recognizing viral RNA with a 5'-triphosphate group (*26*).

The genes are clustered on human chromosome number 10 and contain ISRE elements that bind IRF transcription factors and so can be coordinately induced by the cooperative action of IFNs (*27*).

As previously noted, apoptosis is one of the antiviral mechanisms used during the IFN response. Recently, our laboratory described the role of ISG54 as a mediator of mitochondrial programmed cell death (*28*). Transient transfection of ISG54 in HeLa cells showed a significant increase in apoptosis determined by Propidium Iodide (PI) co-stained with allophycocyanin-annexin V. The work demonstrated that ISG54-induced apoptosis concurred with caspase 3 activation. Caspases are cysteine (cys) proteases responsible for initiating and executing the morphological changes characteristics of apoptosis. BCL-xl, a potent anti-apoptotic protein, reversed the activity of ISG54 in transfection experiments, supporting the conclusion that ISG54 promotes mitochondrial-mediated apoptosis. Glycerol gradient sedimentation identified ISG56 and ISG60 as interactive partners of ISG54 (*28*).

To further understand the molecular pathway involved in the mechanism of ISG54 activity, a two-hybrid yeast screening was performed to identify potential protein interactions with p54. Two antioxidant enzymes were identified in this screen, peroxiredoxin (PRDX) 5 and the superoxide dismutase (SOD) 2. PRDX5 belongs to a family of 6 peroxidases that catalyze the reduction of peroxides, such as hydrogen peroxide and alkyl peroxides. These enzymes protect the cells from the harmful effects of reactive oxygen species. PRDX are functional dimers that use redox-active cysteine residues to reduce peroxides. The reaction is performed in series of steps: first, the thiol group in the peroxidatic cysteine residue (cys-SH) attacks peroxides and becomes oxidized to sulfenic acid (cys-SOH) (*29*) (*30*). The next step in the reaction is performed by a resolving cysteine residue that reacts with the sulfenic acid to form a disulfide

bond. The peroxidases are categorized based on the location of the resolving cysteine residue, that can be located in the opposite subunit of the dimer, on the same polypeptide, or in a different enzyme for 2-cys, atypical 2-cys and 1-cys, respectively. For the final step, thioxiredoxin, a reductase, ultimately reduces the disulfide bond for complete catalysis.

PRDX5 is an atypical 2-cys; the condensation reaction between the two cysteine residues results in the formation of an intra-molecular disulfide bond (*31*). There are three different PRDX5 isoforms generated from different translation initiation sites in gene coding sequence. The first initiation site encodes a transcript variant that localizes in the mitochondria due to a mitochondria targeting sequence (MTS) found in the N-terminus of the protein. A second isoform is localized in the nucleus by a nuclear localization signal; and a third, is expressed in the cytosol and peroxisomes and contains a weak peroxisomal targeting signal type 1 (PTS1) in the C-terminus (*32*) (*33*). PRDX5 has been shown to protect mitochondrial DNA from oxidative stress (*34*) and inhibit p53-mediated apoptosis (*35*).

SOD2 is similarly involved in the clearance of superoxide radicals (*36*). The dismutase catalyzes the detoxification of superoxide radicals in the mitochondria to generate hydrogen peroxide. Peroxides are further detoxified by peroxidases, such as PRDXs (*37*). SOD2 exists endogenously as a homodimer, with the two subunits joined by a disulfide bond. There are three members in the family of SOD. Each member is defined by its cellular localization and catalytic metal. SOD2 is localized in the mitochondrial matrix and contains a manganese metal in its catalytic site (*38*). The biological activity of SOD2 is crucial, demonstrated by gene knockout studies which result in neonatal lethality (*37*). Besides having antioxidant properties, SOD2 has been shown to inhibit cellular actions characteristic of apoptosis, such as TNF-mediated antiproliferative actions and caspase 3 activation (*39*).

The objective of my project was to clone the genes of PRDX5 and SOD2, and confirm the interaction of these two enzymes with p54 by co-immunoprecipitation. Additionally, we assayed the effect of PRDX5 and SOD2 on apoptosis mediated by ISG54 and concluded that the enzymes have a transient regulatory effect on ISG54-mediated apoptosis.

MATERIALS AND METHODS

cDNA Cloning

The cDNA corresponding to human PRDX5 and SOD2 genes (clones, 5166149 and 4184203, respectively) were purchased from Open Biosystems. Two different N-terminal primers were designed to clone the long (1-645 nucleotides) and short (156-645 nucleotides) gene variant of PRDX5 using alternate initiation sites. The long form corresponded to the full length transcript bearing a MTS. The gene variants were cloned using polymerase chain reaction (PCR) into the expression vector pCGN (Addgene) with an N-terminal HA tag downstream of the cytomegalovirus (CMV) promoter and an ampicillin-resistance gene. The primers were designed with N-terminal *X*baI and C-terminal *B*amHI restriction sites and manufactured by Eurofins mwg/operon. The corresponding forward primers used for PCR-amplification of the long and short isoforms cloned into vector pCGN were 5'-CG**TCTAGA**ATGGGACTAGCTGGCGTGTGCGCC-3', and 5'-CG**TCTAGA**ATGGCCCCAATCAAGGTGGGAG-3'. The first codon "ATG" (underlined) corresponds to the first amino acid of the coding sequence and is preceded by the enzyme restriction site (noted in bold). The reverse primer used for both gene variants was 5'-CG**GGATCC**TCAGAGCTGTGAGATGATATTGGG-3'. The last codon TCA (underlined), preceded by the enzyme restriction site (noted in bold), corresponds to the stop codon. In designing the primers, we added CG bases before the restriction enzyme consensus sequence (highlighted in

bold). The “GC clamp” increases efficacy of enzyme binding due to stronger binding of G and C bases. The PCR reaction was performed in a total volume of 50 ul containing 1 U of Platinum Pfx DNA polymerase (Invitrogen) and its recommended buffer, 40 ng of the cDNA template, 10 uM of each primer, 2.5 mM of each deoxynucleotide triphosphates, and 50 mM of MgSO4. Amplification was conducted on a Mastercycler Personal (Eppendorf) using the following conditions: initiation for 2 min at 95 °C, denaturation for 1 min at 95 °C, annealing for 1 min at 55 °C, and elongation for 1.5 min at 72 °C. The cycle was repeated 29 times and with a final elongation step of 10 min at 72 °C.

The PCR products were resolved by gel electrophoresis in ethidium-bromide stained 1 % agarose to confirm successful amplification. The bands corresponding to the vector and the long and short PRDX5 fragments of approximately 645 and 489 base pairs, respectively, were excised from the gel and purified using the Wizard SV Gel and PCR Clean-Up System kit (Promega). Following, we set up a digestion using restriction enzymes purchased from NEBiolabs, recommended buffer NEBuffer 3 suitable for double digest and supplemented with bovine serum albumin. The digestion mixture was set using 1 ul of each restriction enzyme per ug of PCR product in a total volume of 50 ul. After purifying the digested DNA we estimated the ratio of insert to vector qualitatively by gel electrophoresis. The ligation mixture was prepared using a 1:5 ratio of vector/insert, 1 ul of T4 Ligase (Biolabs) in a total volume of 20 ul. Ligation controls were prepared following the same conditions but excluding the PRDX5 inserts. The ligation reaction was carried at 16 °C overnight. E.coli competent cells RapidTrans TAM1 (Active Motif) were transformed with the recombinant plasmid by heat shock. 3 ul of ligation mixture was added to 25 ul of bacterial culture and incubated on ice for 30 min. The cells were heat shocked at 42 °C for 30 seconds. After cooling, 200 ul of SOC broth (super optimal broth with

catabolite repression) was added to the bacterial culture and incubated for 1 hour at 37 °C in a shaker. The cultures were grown in Luria Bertani (*40*). Agar plates were supplemented with 100ug/mL ampicillin overnight at 37 °C. Positive clones were transferred to LB broth supplemented with 100 ug/mL ampicillin and allowed to grow at 37 °C overnight. The bacterial culture was pelleted by centrifugation at 10,000 x g for 5 minutes and the DNA was extracted using Wizard Plus SV Minipreps DNA Purification System protocol (Promega). A 1 ul sample of purified DNA was digested using 0.5 ul of each restriction enzyme in a total volume of 15 ul. The DNA was resolved by gel electrophoresis for confirmation of positive transformation. The DNA was prepared for sequencing by adding 3.2 pmol of primer and was sequenced by the DNA Sequencing Core facility at Stony Brook University. Proper alignment and sequence was analyzed using the program MacVector (Apple).

The gene corresponding to SOD2 was similarly cloned into vector pCGN with N-terminal HA tag. The primers used to clone the gene were: forward 5'-CG**TCTAGA**ATGTTGAGCCGGGCAGTG-'3'and reverse 5'-CG**GGATCC**TCAAACCCATCGAGGCACTCCTTC-3'.

Plasmids

The full-length human ISG54 cDNA was previously cloned into the following vectors:
N-terminal HA tagged pCGN, C-terminal V5 tagged pEF-1V5-HisB (Invitrogen), and C-terminal monomeric GFP tagged pEGFP-N1 (Clontech). pDCR-HRAS-V12 plasmid was a gift from Linda Van Aelst (CSHL).

Cell Culture

HeLa cells were obtained from the American Type Culture Collection. Cells were cultured in Dulbecco's modified Eagle's medium (DMEM) supplemented with 8% Fetal Bovine Serum

(FBS), 1% penicillin (100 U/mL), and streptomycin (100 mg/mL). Cells were incubated at 37 °C with 5 % CO_2.

Transfection

Transfection was performed using TransIT LTI reagent (Mirus) or Polyethanol (PEI) (prepared in-house) at 2 ul and 3 ul per ug of DNA transfected, respectively. For protein expression, cells were cultured in 60 mm plates and transfected with 2 ug of DNA. For co-immunoprecipitation (CO-IP) experiments, cells were cultured in 10 cm plates and transfected with 6 ug of plasmid DNA per sample. Cell medium was replaced one hour prior transfection. The transfection mixture was prepared in 500 ul of serum free DMEM and incubated at room temperature for 15 minutes prior to addition. For endogenous expression of ISG54, cells were treated with 1,000 units of IFN-α 24 hours after transfection. For apoptosis assays, 2.5 $x10^5$ cells/well were seeded in 6-well plates and incubated for 12 hours prior to transfection. The transfection mixture was prepared in 250 ul serum-free DMEM and 2.5-4 ug of total DNA was added per well.

Antibodies

The following commercial antibodies were used at the indicated dilutions for immunodetection and co-immunoprecipitation: mouse monoclonal anti-V5 clone SV5-PK (Invitrogen) 1:1000, polyclonal rabbit anti-HA clone Y-11 (SantaCruz Biotechnology) 1:2000, mouse anti-HA clone 12CA5 (Roche) 1:100, mouse monoclonal anti-PRDX5 clone 12A (Santa Cruz Biotechnology) 1:1000, secondary antibodies for Odyssey Imager: goat anti-mouse IRDye 800, catalog 610-132-121 (Rockland) 1:2000, and goat anti-rabbit Alexa 680, catalog A-21109 (Invitrogen) 1:2500. Secondary antibodies for ECL detection: sheep anti-mouse catalog NA931V (GE Healthcare).

Polyclonal rabbit anti-ISG54 antibodies were generated against the c-terminal region of ISG54 (#1929). Rabbit unspecific serum was used as anti-ISG54 polyclonal rabbit control.

Protein Expression and Co-Immunoprecipitation

To confirm protein expression, HeLa cells transfected with the PRDX5 isoforms and SOD2 were harvested by scraping the monolayer and washed in 1 mL cold PBS. To prevent protein degradation, cells were maintained on ice on all subsequent steps. For protein extraction, cells were pelleted by centrifugation at 2,500 x g for 5 min and lysed using 600 ul of high salt 0.5% Nonidet P-40 lysing buffer (400 mM NaCl, 50 mM Tris-pH 7.5, 5 mM EDTA, 50 mM NaF, 10 % glycerol). A mixture of protease inhibitors was added to the lysing buffer: phenylmethylsulfonyl fluoride (PMSF) diluted 1:100, and a mammalian protease inhibitor cocktail (Sigma), diluted 1:1000. Cells were pipetted vigorously and incubated on a rotary shaker for 30 min at 4° C. To collect lysates, cells were centrifuged at 14,000 x g for 15 min at 4° C. To calculate protein concentration, 2 ul of lysate was diluted 1:5 with water and added 1 mL of 1x solution of Protein Assay reagent (BioRad). The solutions were read in a spectrophotometer at 595 wavelength. Calculations were performed by plotting the absorbance values versus concentration in an excel graph using a set of standards prepared with BSA. The protein concentration was determined by dividing the absorbance by the y-intercept value generated from the standard plot. The concentration of protein used was calculated from the most diluted sample and divided into two equal parts for test and control. The lysates were diluted 1:2 in 2x sample buffer and heated at 95 °C for 10 min.

Proteins were separated by SDS-PAGE in 10-12 % polyacrylamide gel and transferred to nitrocellulose membrane (Fisher). For immunodetection, membrane blots were blocked in fresh

5 % milk diluted in TRIS buffered saline with Tween-20 at 1:1000 (TBST) for 1 hour at 4 °C rotating. Antibodies were diluted in blocking buffer and all incubations were performed at 4 °C rotating. After blocking, blots were washed three times with TBST, each wash consisting of 10 minutes incubation with medium shaking. Primary antibody was subsequently added and incubated overnight. Finally, after washing the blots as described, secondary antibody was added and incubated for 1 hour.

The substrate solution for ECL detection was prepared immediately before adding to the blot, and allowed to react for 1 minute. The blots were placed in protective plastic and transferred to an ECL cassette. A film was placed on top of the blot and incubated in the cassette protected from light. First exposure was performed at 30 second and increased until optimal signal was obtained. The films were developed by Enhanced chemiluminescence (ECL, Thermo Scientific). Films were scanned to generate digital images. The Odyssey Imager (LI-COR) was used for near-infrared fluorescent detection. Images were analyzed using Image J software (NIH).

For co-immunoprecipitation, cell lysates were collected and divided into two equal parts, yielding 40-100 ug of whole-cell lysate for test and control samples. Prior to antibody incubation, cell lysates were pre-cleared by using 10 ul of protein-G agarose (Invitrogen) and incubated for 15 minutes at 4° C. The beads were pelleted by centrifugation and the cleared lysate transferred to a new tube. Indicated antibodies were added to the lysates and incubated for 4 hours at 4° C rotating. Protein G agarose beads were blocked prior to adding it to the lysates by resuspending the beads in 5 % BSA/PBS solution and incubating for 30 min rotating. The beads were subsequently washed 3 times with PBS and 20 ul was added to each sample. Immunocomplexes were washed 3 times with 1 mL bead wash buffer (1:1 lysing buffer diluted with a low salt concentration solution of 10 mM NaCl, 10 mM TRIS pH 7). The

immunocomplexes were resuspended in 50 ul 2x of denaturing sample buffer. Co-immunoprecipitation samples were separated by SDS-PAGE in 10-12 % polyacrylamide gel, immunoblotted and detected as mentioned above.

Apoptosis Assessment

For apoptosis assessment, experiment readouts were performed 24, 48, and 72 hours post transfection. The cell medium was transferred to 5 mL culture tubes. Adherent cells were harvested using TrypLE Express (Life Technologies) and combined with cells in suspension previously collected. Cells were pelleted by centrifugation at 1,500 x g for 5 minutes and washed with Phosphate Buffered Saline (PBS). Cells were co-stained with Annexin V conjugated to allophycocyanin (APC) (BD Pharmigen) and Propidium Iodide (PI) (Invitrogen). A 10x concentration of Annexin V binding buffer was prepared in-house as per manufacturing instructions (0.1 M Hepes (pH 7.4) 1.4 M NaCl, 25 mM $CaCl_2$). The 1mg/mL stock of PI was diluted 1:1000 in Annexin V binding buffer. Cells were resuspended in 100 ul of PI/Annexin binding buffer, added 5 ul of Annexin V APC antibody and pipetted gently to mix. The tubes were incubated in dark at room temperature for 15 minutes and the volume was adjusted to 500 ul with PI/Annexing binding buffer. Flow cytometric analysis was performed in a FacsCalibur flow cytometer (BD Biosciences). The gate was set for GFP expression, for selective analyzes of ISG54-transfected population. 10,000 cells in each population were analyzed with BD CellQuest software.

RESULTS

Molecular cloning and protein expression of PRDX5 isoforms- To study the interaction of p54 with PRDX5 screened in a yeast-two-hybrid assay, two isoforms of PRDX5 were recombinantly cloned by PCR (Fig 3A). The cDNA corresponding to human PRDX5 gene was cloned into vector HA-pCGN, using the restriction enzymes *Xba*I and *Bam*HI (Fig 3B). The primers were designed to generate a longer isoform, PRDX5 L, containing a mitochondrial targeting signal (MTS) in the 5' end. The MTS was omitted in the short variant, PRDX5 S, to generate expression of the isoform localized in the cytosol and peroxisomes. The resulting recombinant proteins contained an HA tag in the N' terminus. The expression of the proteins was driven by CMV promoter for expression in HeLa cells (Fig 3B). The PCR product obtained from the amplification were approximately 645 bp and 489 bp corresponding to the long and short gene isoforms, respectively (Fig 4). Protein expression of both plasmids was confirmed by Western blotting. The protein bands analyzed had a molecular mass of approximately 25 kDa and 18 kDa for PRDX5 L and PRDX5 S, respectively (Fig 5). Notably, the expression of the mitochondrial isoform PRDX5 L was stronger than PRDX5 S.

Interaction of PRDX5 with ISG54 isoforms and ISG60- After confirming cloning and protein expression, we performed a co-immunoprecipitation of ISG54 with the genes cloned. Transient transfection of plasmids coding for both isoforms of PRDX5 was performed together with plasmids coding for p54 or its interactive partner, p60. The protein interaction was analyzed by co-immunoprecipitation and Western blot (Fig 6). The results confirmed interaction of p54 with PRDX5 L, but not with PRDX5 S. Interestingly, p60, co-immunoprecipitated with both isoforms of PRDX5. The interaction of PRDX5 L was significantly stronger with p60 than with p54.

Western blots of straight lysates showed the input levels of PRDX5 S slightly greater than PRDX5 L.

Endogenous ISG54 interacts with transiently transfected PRDX5- To determine if the interaction of ISG54 with PRDX5 L was a result of overexpressed protein, HeLa cells were treated with IFN-α to induce endogenous expression of ISG54 to assess interaction with transiently transfected PRDX5 isoforms. Treatment with IFN-α was performed 24 hours after transfection and cells were subsequently incubated for an additional 8 hours prior to harvest. Endogenous p54 was immunoprecipitated using anti-54 antibodies and Western blot was performed with anti-PRDX5 (Fig 7A). Since antibody to PRDX5 reacts with both the transfected protein and the endogenous PRDX5 protein, multiple bands were detected in the lysate from HA-pCGN vector controls. Binding of p54 to PRDX5 L and PRDX5 S was detected although there was stronger binding between PRDX5 L and p54. The experiment was repeated (Fig 7B) with anti-HA antibody to detect only the transfected PRDX5 protein; expression of endogenous p54 was induced by treating the cells with IFN-α. The interaction between endogenous p54 with transfected PRDX5 L was confirmed.

Effects of PRDX5 on ISG54-mediated apoptosis- To evaluate the possibility that PRDX5 could reduce ISG54-mediated apoptosis, HeLa cells were transfected with plasmids coding for ISG54 and PRDX5 and examined for apoptosis by performing Annexin V and PI staining flow cytometric analysis. Apoptotic levels of HeLa cells co-transfected with ISG54 and PRDX5 isoforms were compared to the levels seen in ISG54 expressing cells. Monomeric-GFP (mono-GFP) was used as baseline control. During the initial stage of apoptosis, a characteristic loss of membrane integrity causes phosphatidylserine (PS) to translocate from the inner to outer

membrane exposing the phospholipids to the extracellular environment. Annexin V is a phospholipid binding protein that binds with increased affinity to exposed PS and is used as a marker for apoptosis. PI is another marker used to study apoptotic and necrotic cells. PI is a fluorescent molecule that intercalates between the bases of DNA. During later stages of apoptosis and in necrosis, the nuclear envelope disintegrates allowing the dye to bind to DNA. Apoptosis assessment was performed on cells expressing ISG54-monomeric GFP. Approximately 50 % of cells expressing ISG54-monomeric GFP alone were seen to undergo cell death by 48 hours; with levels increasing above 70 % at 72 hours, concordant with previously reported data (*28*). PRDX5 S inhibited ISG54-mediated apoptosis at 24 hours by 50 % determined by Annexin V staining (Fig 8A). The levels of PI staining of ISG54 expressing cells with and without PRDX5 in the early time periods were within 10 % (Fig 8B). PRDX5 isoforms did not influence the apoptosis induced by p54 at 48 or 72 hours.

SOD2 interaction with p54- SOD2, the second antioxidant enzyme detected in the yeast-two-hybrid assay with ISG54 was similarly cloned into vector HA-pCGN and pEF1-V5. The cloning was performed using enzymes *Xba*I and *Bam*HI (9). The PCR amplification confirmed a gene product of approximately 423 bp for both HA-SOD2 (Fig 10). Protein expression of HA-SOD2 was performed by transient transfection in HeLa cells and Western blotting. The results showed two bands corresponding to approximately 16 kDa molecular weight. The bands could possibly represent the dimeric form of SOD2 (Fig 11). Co-immunoprecipitation was conducted to confirm the protein-protein interaction of SOD2 and p54. HeLa cells were transfected with HA-SOD2, and endogeneous p54 was induced with IFN-α treatment. Western blotting using anti-HA antibody confirmed the interaction of HA-SOD2 with endogeneous p54 (Fig 12).

Regulation of p54-mediated apoptosis by SOD2- With the objective of identifying molecular partners of p54 that regulate its activity as a promoter of apoptosis, we repeated the apoptosis assessment of HeLa cells transiently transfected with HA-SOD2 and ISG54monoGFP plasmids. *HA*-SOD2 reduced p54-induced apoptosis by 50 % at 24 hour, demonstrated by annexin-V and PI staining (Fig 13). Since the transfection procedure can induce a basal level of cell death, we used a monomeric-GFP condition as a baseline level control. The inhibitory effects mediated by SOD2 on apoptosis decreased by 48 hours to 10 % versus p54. By 72 hours, SOD2 levels were close to the levels of p54.

DISCUSSION

The IFN system plays a major role in innate and adaptive immunity during viral infection. IFN antiviral response is mediated by the expression of interferon stimulated genes (ISG) that mediate cellular responses to protect the host against infection. There are different classes of IFN, based on sequence homology and receptor specificity. Type I IFN, includes IFN-α and IFN-β, which are part of the first wave of cytokines expressed upon a viral infection. ISG54 is part of the IFIT family of ISG that is expressed in response to type I IFN signaling.

Based on recent laboratory findings indicating that ISG54 gene product, p54, induces apoptosis, we investigated if the interaction identified in a yeast-two-hybrid screening between p54 with PRDX5 and SOD2, mediated such activity. PRDX5 and SOD2 are antioxidant enzymes that protect the cells against the effect of reactive oxygen species. To confirm the interaction between p54 and these two enzymes, we cloned the cDNA corresponding to PRDX5 short and long variants (PRDX5 S and PRDX5 L) and SOD2 by PCR.

We detected distinct signal patterns of protein expression between PRDX5 isoforms. The protein level detected for PRDX5 S was greater than the level of PRDX5 L. The result might due to increased protein expression or stability of mRNA transcript of PRDX5 S. We confirmed the interaction between overexpressed p54 and PRDX5 isoforms, as well as with SOD2. In addition, we determined that this expression was not due to overexpression of p54 in transient transfection by confirming protein-protein interaction of endogenous p54 with PRDX5 L, PRDX5 S and SOD2. Based on our results, the interaction between endogenous p54 and the mitochondrial isoform, PRDX5 L, was stronger than with the PRDX5 S. It is possible that p54 is localized near the mitochondria resulting in stronger binding of p54 to mitochondrial PRDX5.

We assayed the effect of these antioxidants on ISG54-mediated apoptosis. Our results show for the first time the regulatory function of PRDX5 and SOD2 on the activity induced by ISG54. We determined that although partial, both enzymes had a transient regulatory role on ISG54 activity. Both isoforms of PRDX5 reduced cell death induced by p54 at 24 hours post transfection and SOD2 reduced the activity of p54 for 48 hours post transfection. These findings shed light in the molecular mechanism involved in ISG54 activity. Regulation of PRDX5 activity by these antioxidants is shown to be a transient event, which exemplifies the tight regulation of IFN-mediated events necessary to maintain cellular homeostasis. Based on our results showing regulation of these antioxidants in a 24-48 hour period, further work will look closer at the events occurring within a 48 hour period post transfection.

Additional investigation is necessary to elucidate the biological significance of this interaction, which could signify a regulation of the activity of PRDX5 and SOD2 by ISG54. Since the effect of ISG54 prominently promotes apoptosis, it is possible that ISG54 reduces the activity of PRDX5 and SOD2 and reduces the cells defense against oxidative stress. Future work will focus

in studying the interaction of ISG54 with these antioxidants, such as mapping the protein interaction domains and determining the cellular localization of such interactions. It would be interesting to determine if both PRDX5 and SOD2 can interact with p54 simultaneously, or if they recognize the same binding domain. In addition, we will also determine if the interactive partners of ISG54, ISG56 and ISG60, also recognize PRDX5 and SOD2.

FIGURES

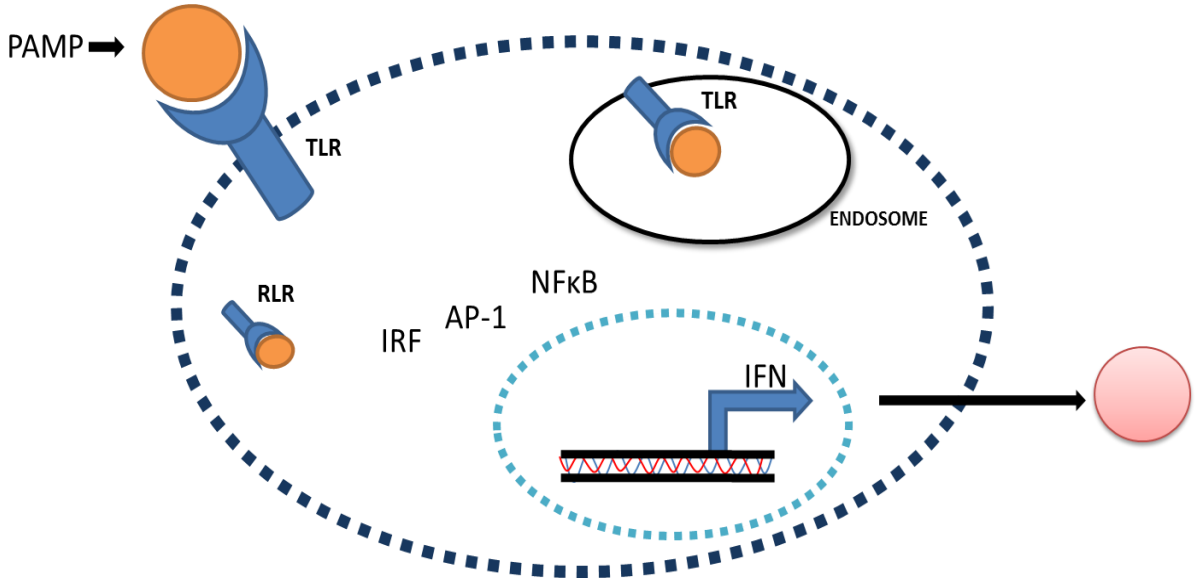

Figure 1 TLR and RLR recognition of PAMP leading to transcriptional activation of type I/II IFN gene expression

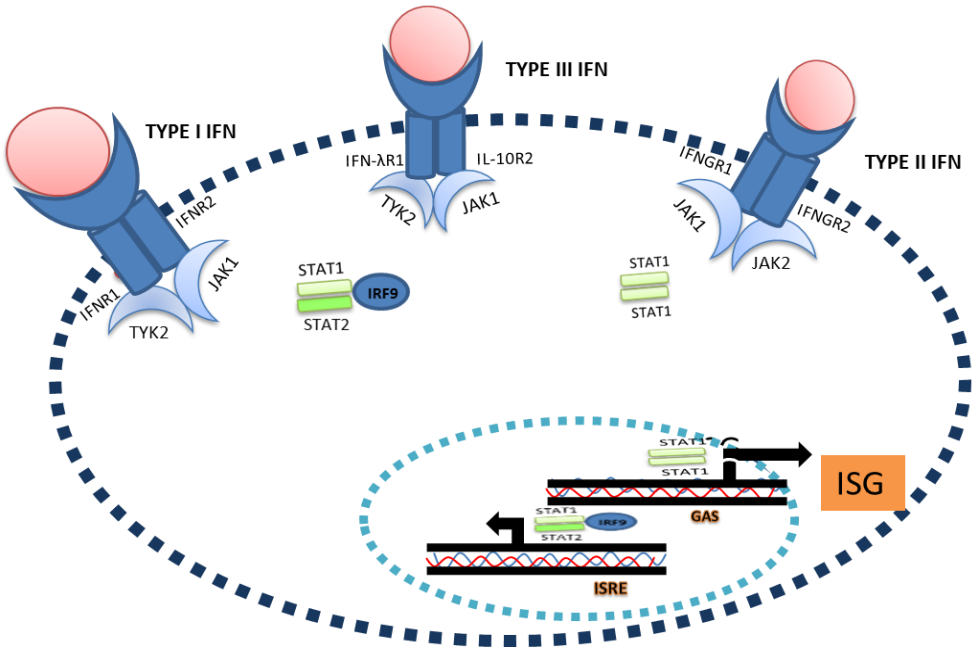

Figure 2 Signal transduction pathways of IFN
Following ligation of cell surface receptors, associated JAKs activate STAT complexes. Type I and type III IFN activate the ISGF3 complex composed of STAT1 and STAT2 dimer and IRF9. TYPE II IFN activates the STAT1 homodimer. The transcription complexes enter the nucleus and induce expression of ISG.

A

```
  1 cgcgcctgcg cagtggaggc ggcccaggcc cgccttccgc agggtgtcgc cgctgtgccg
 61 ctagcggtgc cccgcctgct gcggtggcac cagccaggag gcggagtgga agtggccgtg
121 gggcgggtat gggactagct ggcgtgtgcg ccctgagacg ctcagcgggc tatatactcg
181 tcggtggggc cggcggtcag tctgcggcag cggcagcaag acggtgcagt gaaggagagt
241 gggcgtctgg cggggtccgc agtttcagca gagccgctgc agccatggcc ccaatcaagg
301 tgggagatgc catcccagca gtggaggtgt ttgaagggga gccagggaac aaggtgaacc
361 tggcagagct gttcaagggc aagaagggtg tgctgtttgg agttcctggg gccttcaccc
421 ctggatgttc caagacacac ctgccagggt ttgtggagca ggctgaggct ctgaaggcca
481 agggagtcca ggtggtggcc tgtctgagtg ttaatgatgc ctttgtgact ggcgagtggg
541 gccgagccca caaggcggaa ggcaaggttc ggctcctggc tgatcccact ggggcctttg
601 ggaaggagac agacttatta ctagatgatt cgctggtgtc catctttggg aatcgacgtc
661 tcaagaggtt ctccatggtg gtacaggatg gcatagtgaa ggccctgaat gtggaaccag
721 atggcacagg cctcacctgc agcctggcac ccaatatcat ctcacagctc tgaggccctg
781 ggccagatta cttcctccac ccctccctat ctcacctgcc cagccctgtg ctggggccct
841 gcaattggaa tgttggccag atttctgcaa taaacacttg tggtttgcgg ccatctcctt
901 ggttaaaaaa aaa
```

B

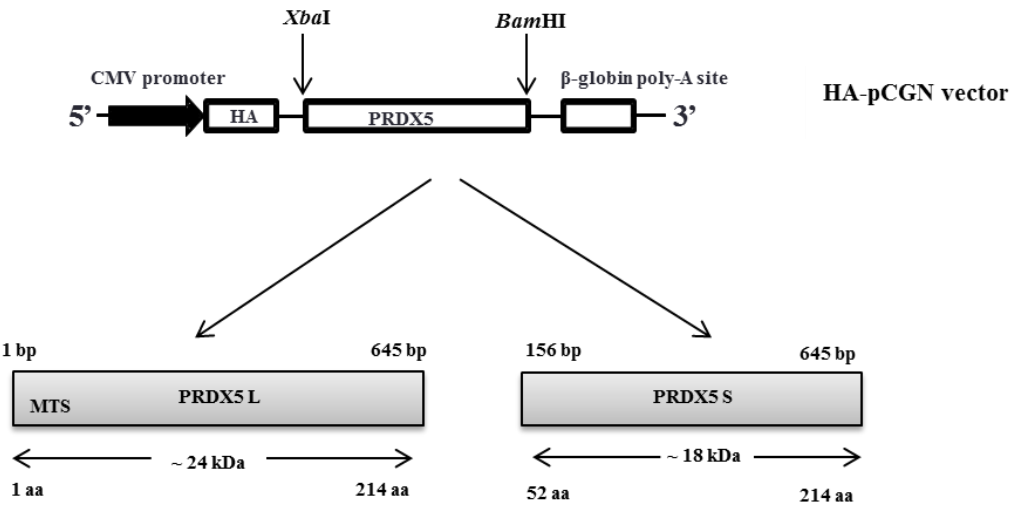

Figure 3 Nucleotide sequence corresponding to human PRDX5 gene and plasmid design
We cloned the cDNA of PRDX5 corresponding to two isoforms into vector HA-pCGN. (A) The coding sequence of the gene contains alternate translation initiation sites that code for isoforms with different cellular localization. The alternate initiation sites represented by the start codon "ATG" are shown underlined. (B) Gene vector design showing a diagram of plasmid containing the gene coding for PRDX5 long (PRDX5 L) or PRDX5 short (PRDX5 S). PRDX5 L sequence corresponds to 1-645 basepairs (bp), coding for amino acids (aa) 1-214. PRDX5 S sequence corresponds to 156-645 bp, coding for 52-214 aa. The gene product molecular weight for PRDX5 L and PRDX5 S is approximately 24 and 18 kDa, respectively.

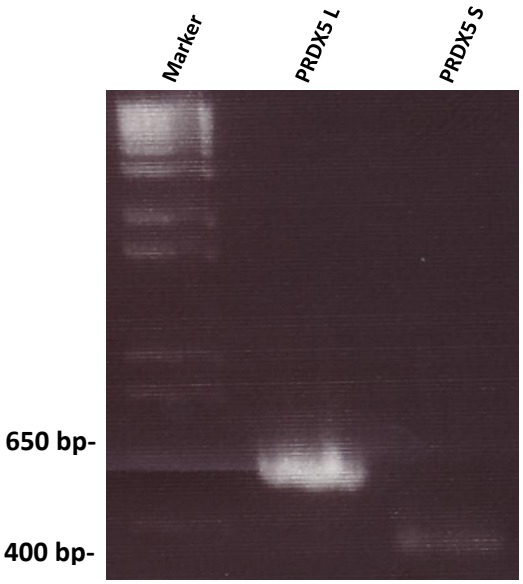

Figure 4 Ethidium bromide-stained agarose gel of PCR products corresponding to PRDX5 L and PRDX5 S

Two isoforms of the human PRDX5 gene were amplified by PCR. The PCR products were resolved by electrophoresis in 1 % agarose gel stained with ethidium bromide. The molecular mass marker shown on the left was used to estimate the molecular size of amplified DNA to confirm target gene amplification. The PCR products resolved corresponded to PRDX5 L (645 bp) and PRDX5 S (489 bp).

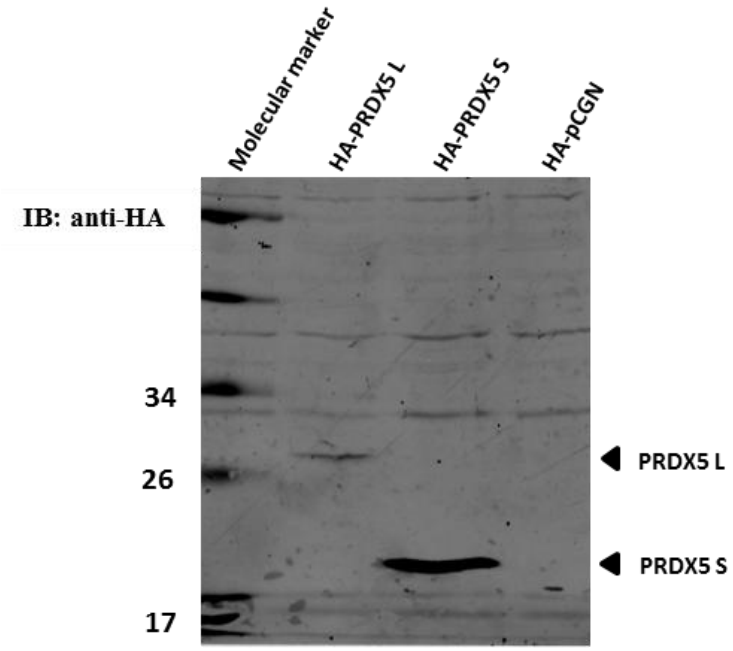

Figure 5 Protein expression of transiently transfected PRDX5 L and PRDX5 S

HeLa cells were transfected with plasmids coding for HA-PRDX5 L, HA-PRDX5 S, and empty vector control (HA-pCGN). Cells were harvested 24 hours after transfection and whole cell extracts were collected. Proteins were resolved by SDS-PAGE and Western blot using monoclonal anti-HA antibody. The molecular weight standards are shown on the left in kDa.

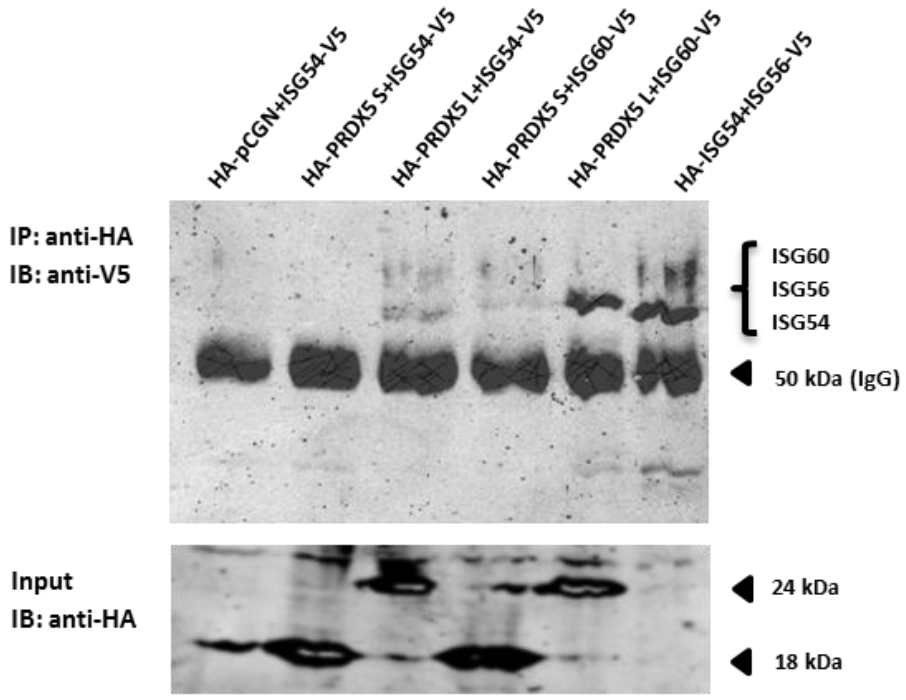

Figure 6 Co-immunoprecipitation of transiently transfected PRDX5 isoforms with ISG54 or ISG60
Hela cells were transfected with PRDX5 isoforms with and without plasmids coding for ISG54 and ISG60. After 24 hours, cells were harvested and 475 ug of whole-cell lysates were co-immunoprecipitated with anti-HA antibody. Protein determination of the immunocomplexes and whole-cell lysates was performed by SDS-PAGE and Western blotting. Transfection of ISG54 with HA-pCGN (empty vector) and ISG54 with ISG60 were used as negative and positive controls, respectively.

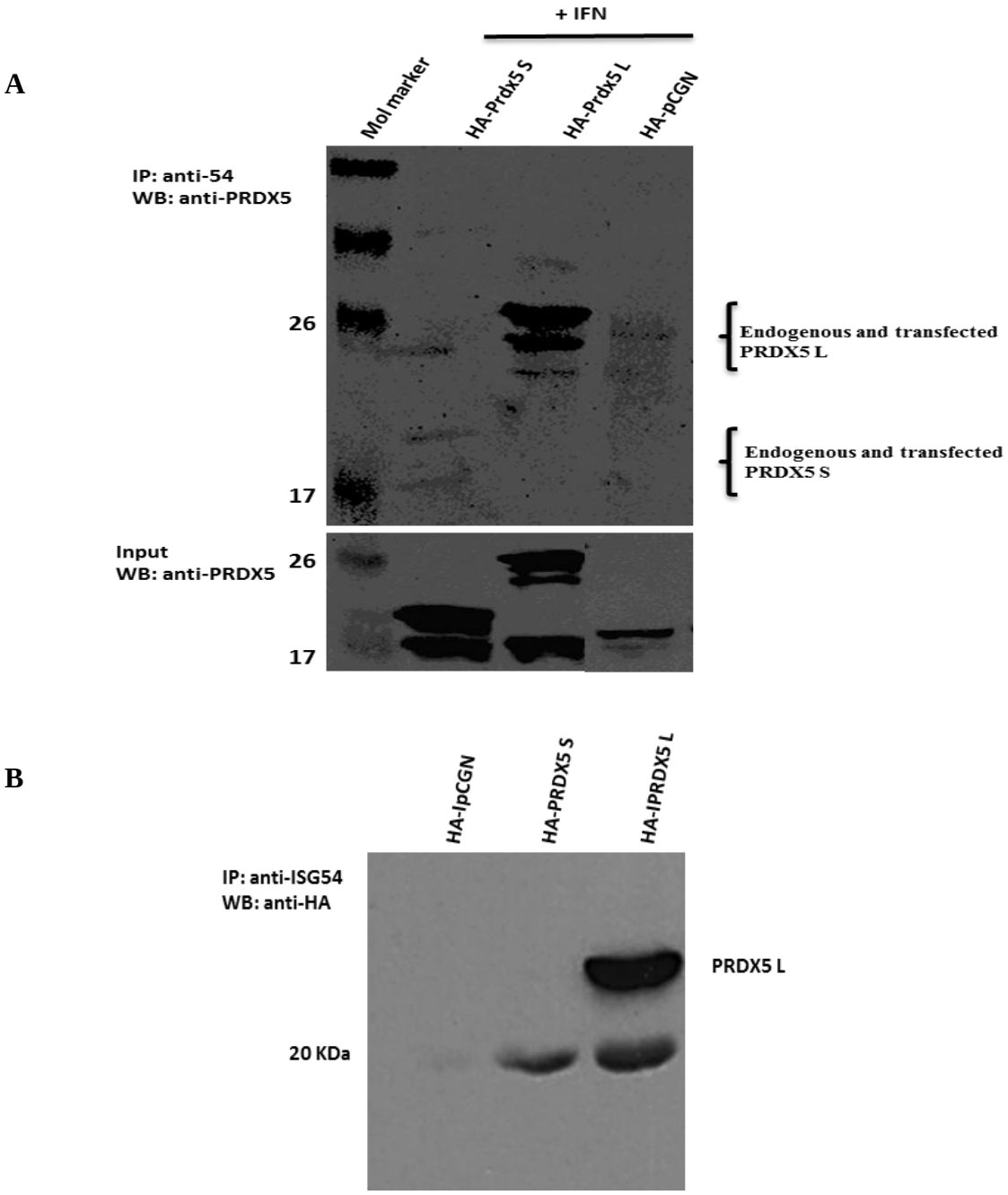

Figure 7 Co-immunoprecipitation of transiently transfected PRDX5 isoforms with endogenous ISG54

To examine whether overexpressed PRDX5 L and PRDX5 S can interact with endogenous ISG54, HeLa cells were transfected with plasmids coding for the indicated genes and treated with IFN-α. (A) 500 ug of protein lysate were immunoprecipitated with anti-PRDX5 antibody and blotted with anti-HA. (B) The experiment was repeated using 375 ug of protein lysate co-immunoprecipitated with anti-ISG54 and blotted with anti-HA antibody. The IgG light chain band is noted on the left as 20 kDa.

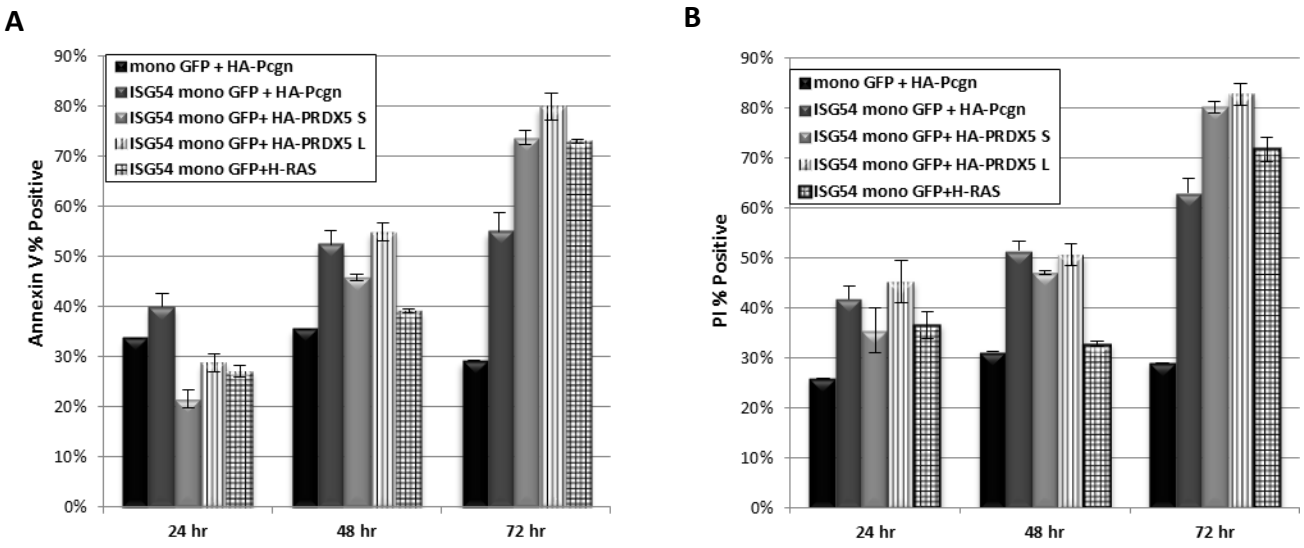

Figure 8 PRDX5 regulation of ISG54-mediated apoptosis

To investigate if PRDX5 interaction with ISG54 regulated the mechanism of ISG54-mediated apoptosis, we performed Annexin V/PI staining of HeLa cells co-transfected with the indicated plasmids and analyzed cells by flow cytometry. A total of 2.5 ug of DNA was transfected per well using Mirus reagent. Cells were harvested and stained at 24, 48 and 72 hours post transfection.

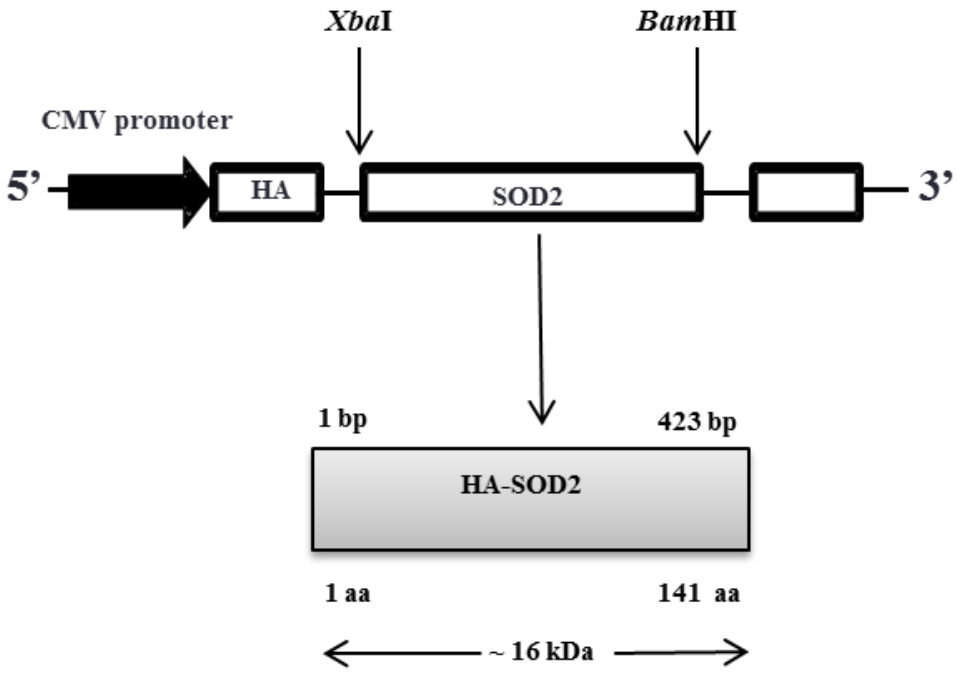

Figure 9 SOD2 plasmid design
The diagram shows the plasmid containing the gene coding for SOD2 cloned into vector HA-pCGN bearing a N-terminal HA tag. The first amino acid corresponds to the start codon "ATG." The sequence corresponds to 1-423 basepairs (bp), coding for amino acids (aa) 1-141. The HA-SOD2 gene product has a predicted molecular weight of 16 kDa.

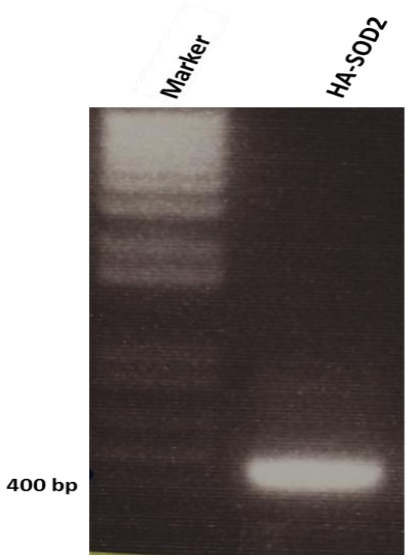

Figure 10 Ethidium bromide-stained agarose gel of PCR product corresponding to HA-SOD
The gene coding for antioxidant SOD2 (423 bp) was cloned by PCR. The PCR product was resolved by electrophoresis in 1 % agarose gel stained with ethidium bromide. The molecular marker shown on the left was used to estimate the molecular size of amplified DNA to confirm target gene amplification.

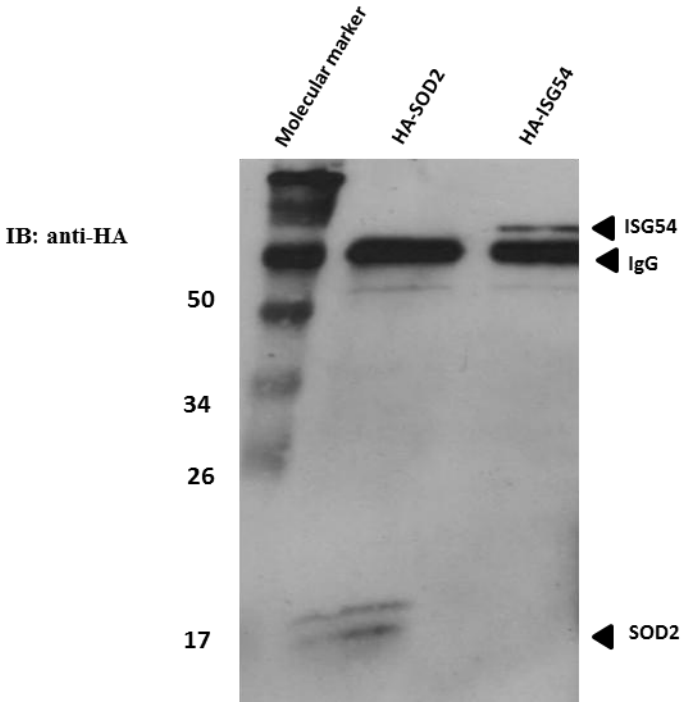

Figure 11 Protein expression profile of transiently transfected SOD2
Recombinant plasmid coding for HA-SOD2 was transfected in HeLa cells. The proteins were resolved in SDS-PAGE and detected by Western blot using anti-HA antibody. The molecular standards are shown on the left (kDa). Transfection of HA-ISG54 and HA-pCGN were used as controls.

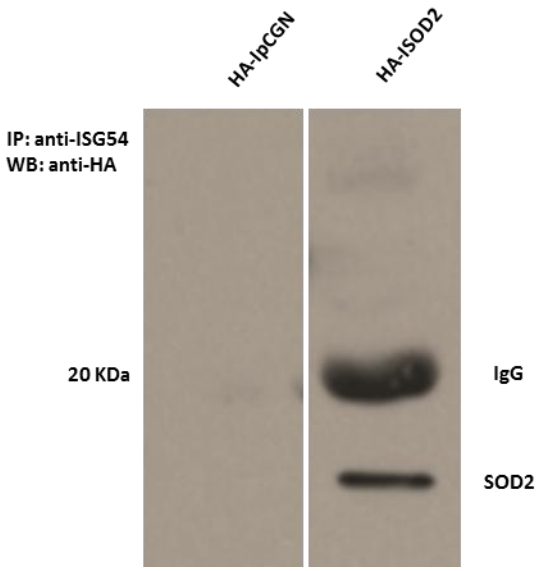

Figure 12 Co-immunoprecipitation of transiently transfected HA-SOD2 with endogenous ISG54
To examine whether overexpressed HA-SOD2 can interact with endogenous p54, HeLa cells were transfected with the indicated plasmids and treated with IFN-α. 375 ug of protein lysate was immunoprecipitated with anti-54 antibody and blotted with anti-HA antibody.

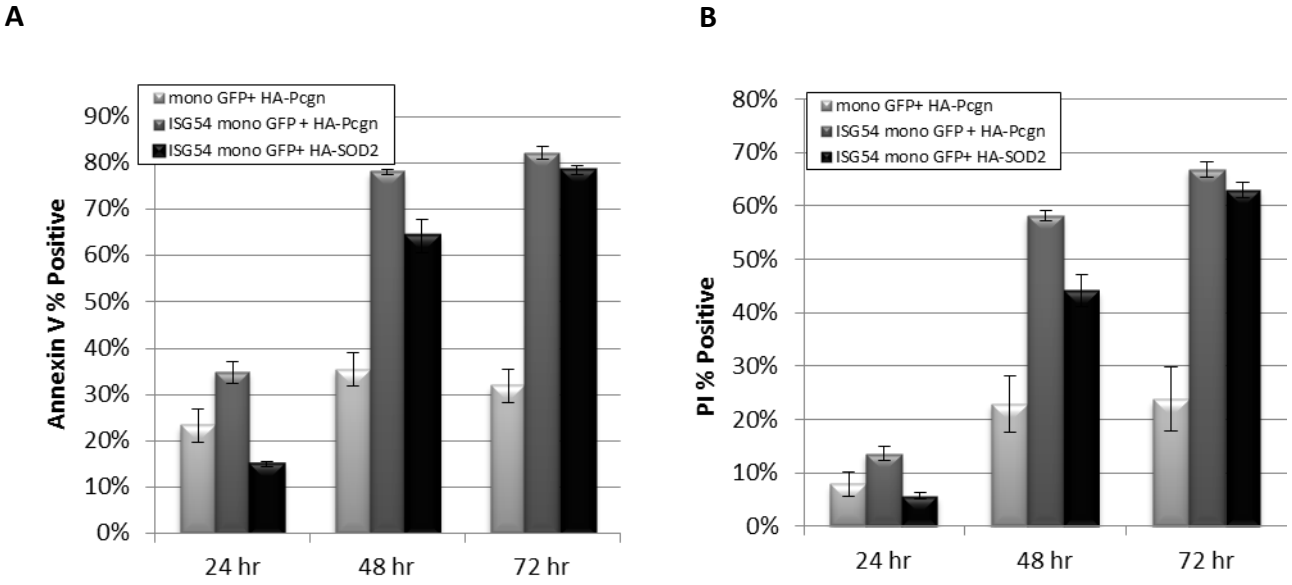

Figure 13 SOD2 reduces cell death induced by p54
HeLa cells were transfected with plasmids coding for ISG54monoGFP with and without HA-SOD2 and incubated for 24, 48 and 72 hours. Harvested cells were stained with Annexin V/PI for apoptotic assessment. Apoptosis was determined by gating the GFP positive population to analyze cells expressing ISG54. The left and right panels show percentage of GFP-positive cells stained for Annexin and PI, respectively.

REFERENCES

1. G. C. Sen, Viruses and interferons. *Annual review of microbiology* **55**, 255 (2001).
2. L. Malmgaard, Induction and regulation of IFNs during viral infections. *Journal of interferon & cytokine research : the official journal of the International Society for Interferon and Cytokine Research* **24**, 439 (Aug, 2004).
3. L. C. Platanias, Mechanisms of type-I- and type-II-interferon-mediated signalling. *Nature reviews. Immunology* **5**, 375 (May, 2005).
4. A. Lasfar, W. Abushahba, M. Balan, K. A. Cohen-Solal, Interferon lambda: a new sword in cancer immunotherapy. *Clinical & developmental immunology* **2011**, 349575 (2011).
5. S. Joshi *et al.*, Type I interferon (IFN)-dependent activation of Mnk1 and its role in the generation of growth inhibitory responses. *Proceedings of the National Academy of Sciences of the United States of America* **106**, 12097 (Jul 21, 2009).
6. S. Jensen, A. R. Thomsen, Sensing of RNA viruses: a review of innate immune receptors involved in recognizing RNA virus invasion. *Journal of virology* **86**, 2900 (Mar, 2012).
7. N. C. Reich, Nuclear/cytoplasmic localization of IRFs in response to viral infection or interferon stimulation. *Journal of interferon & cytokine research : the official journal of the International Society for Interferon and Cytokine Research* **22**, 103 (Jan, 2002).
8. T. Decker, IFNs and STATs in innate immunity to microorganisms. *Journal of Clinical Investigation* **109**, 1271 (2002).
9. U. Senftleben *et al.*, Activation by IKKalpha of a second, evolutionary conserved, NF-kappa B signaling pathway. *Science* **293**, 1495 (Aug 24, 2001).
10. T. Kawai, S. Akira, Toll-like receptor and RIG-I-like receptor signaling. *Annals of the New York Academy of Sciences* **1143**, 1 (Nov, 2008).
11. N. Yan, Z. J. Chen, Intrinsic antiviral immunity. *Nature immunology* **13**, 214 (Mar, 2012).
12. Y. Kumagai, S. Akira, Identification and functions of pattern-recognition receptors. *The Journal of allergy and clinical immunology* **125**, 985 (May, 2010).
13. M. A. Delgado, V. Deretic, Toll-like receptors in control of immunological autophagy. *Cell death and differentiation* **16**, 976 (Jul, 2009).
14. O. Schulz *et al.*, Protein kinase R contributes to immunity against specific viruses by regulating interferon mRNA integrity. *Cell host & microbe* **7**, 354 (May 20, 2010).
15. S. Uematsu, S. Akira, Toll-Like receptors (TLRs) and their ligands. *Handbook of experimental pharmacology*, 1 (2008).
16. H. Tsujimura *et al.*, Toll-like receptor 9 signaling activates NF-kappaB through IFN regulatory factor-8/IFN consensus sequence binding protein in dendritic cells. *J Immunol* **172**, 6820 (Jun 1, 2004).
17. J. Lund, A. Sato, S. Akira, R. Medzhitov, A. Iwasaki, Toll-like receptor 9-mediated recognition of Herpes simplex virus-2 by plasmacytoid dendritic cells. *The Journal of experimental medicine* **198**, 513 (Aug 4, 2003).
18. C. Schindler, D. E. Levy, T. Decker, JAK-STAT signaling: from interferons to cytokines. *The Journal of biological chemistry* **282**, 20059 (Jul 13, 2007).
19. G. Banninger, N. C. Reich, STAT2 nuclear trafficking. *The Journal of biological chemistry* **279**, 39199 (Sep 17, 2004).
20. G. Gastl, C. Huber, The biology of interferon actions. *Blut* **56**, 193 (May, 1988).

21. K. Schroder, P. J. Hertzog, T. Ravasi, D. A. Hume, Interferon-gamma: an overview of signals, mechanisms and functions. *Journal of leukocyte biology* **75**, 163 (Feb, 2004).
22. G. L. Blatch, M. Lassle, The tetratricopeptide repeat: a structural motif mediating protein-protein interactions. *BioEssays : news and reviews in molecular, cellular and developmental biology* **21**, 932 (Nov, 1999).
23. L. D. D'Andrea, L. Regan, TPR proteins: the versatile helix. *Trends in biochemical sciences* **28**, 655 (Dec, 2003).
24. T. Horibe, M. Kohno, M. Haramoto, K. Ohara, K. Kawakami, Designed hybrid TPR peptide targeting Hsp90 as a novel anticancer agent. *Journal of translational medicine* **9**, 8 (2011).
25. F. Terenzi, C. White, S. Pal, B. R. Williams, G. C. Sen, Tissue-specific and inducer-specific differential induction of ISG56 and ISG54 in mice. *Journal of virology* **81**, 8656 (Aug, 2007).
26. A. Pichlmair *et al.*, IFIT1 is an antiviral protein that recognizes 5'-triphosphate RNA. *Nature immunology* **12**, 624 (Jul, 2011).
27. V. Fensterl, G. C. Sen, The ISG56/IFIT1 gene family. *Journal of interferon & cytokine research : the official journal of the International Society for Interferon and Cytokine Research* **31**, 71 (Jan, 2011).
28. M. Stawowczyk, S. Van Scoy, K. P. Kumar, N. C. Reich, The interferon stimulated gene 54 promotes apoptosis. *The Journal of biological chemistry* **286**, 7257 (Mar 4, 2011).
29. M. Trujillo *et al.*, Pre-steady state kinetic characterization of human peroxiredoxin 5: taking advantage of Trp84 fluorescence increase upon oxidation. *Archives of biochemistry and biophysics* **467**, 95 (Nov 1, 2007).
30. S. G. Rhee, H. A. Woo, I. S. Kil, S. H. Bae, Peroxiredoxin functions as a peroxidase and a regulator and sensor of local peroxides. *The Journal of biological chemistry* **287**, 4403 (Feb 10, 2012).
31. C. Evrard *et al.*, Crystal structure of a dimeric oxidized form of human peroxiredoxin 5. *Journal of molecular biology* **337**, 1079 (Apr 9, 2004).
32. Z. A. Wood, E. Schroder, J. Robin Harris, L. B. Poole, Structure, mechanism and regulation of peroxiredoxins. *Trends in biochemical sciences* **28**, 32 (Jan, 2003).
33. A. Kropotov, N. Usmanova, V. Serikov, B. Zhivotovsky, N. Tomilin, Mitochondrial targeting of human peroxiredoxin V protein and regulation of PRDX5 gene expression by nuclear transcription factors controlling biogenesis of mitochondria. *The FEBS journal* **274**, 5804 (Nov, 2007).
34. I. Banmeyer, C. Marchand, A. Clippe, B. Knoops, Human mitochondrial peroxiredoxin 5 protects from mitochondrial DNA damages induced by hydrogen peroxide. *FEBS letters* **579**, 2327 (Apr 25, 2005).
35. Y. Zhou *et al.*, Mouse peroxiredoxin V is a thioredoxin peroxidase that inhibits p53-induced apoptosis. *Biochemical and biophysical research communications* **268**, 921 (Feb 24, 2000).
36. Y. Zhou *et al.*, Bacterial scavengase p20 is structurally and functionally related to peroxiredoxins. *Biochemical and biophysical research communications* **233**, 848 (Apr 28, 1997).
37. C. Liu, D. Ogando, J. A. Bonanno, SOD2 contributes to anti-oxidative capacity in rabbit corneal endothelial cells. *Molecular vision* **17**, 2473 (2011).

38. I. N. Zelko, T. J. Mariani, R. J. Folz, Superoxide dismutase multigene family: a comparison of the CuZn-SOD (SOD1), Mn-SOD (SOD2), and EC-SOD (SOD3) gene structures, evolution, and expression. *Free radical biology & medicine* **33**, 337 (Aug 1, 2002).
39. S. K. Manna, H. J. Zhang, T. Yan, L. W. Oberley, B. B. Aggarwal, Overexpression of manganese superoxide dismutase suppresses tumor necrosis factor-induced apoptosis and activation of nuclear transcription factor-kappaB and activated protein-1. *The Journal of biological chemistry* **273**, 13245 (May 22, 1998).
40. R. S. Longman *et al.*, Dendritic-cell maturation alters intracellular signaling networks, enabling differential effects of IFN-alpha/beta on antigen cross-presentation. *Blood* **109**, 1113 (Feb 1, 2007).